Cloud condensation nucleus activation properties of biogenic secondary organic aerosol

Timothy M. VanReken
National Center for Atmospheric Research, Boulder, Colorado, USA

Nga L. Ng, Richard C. Flagan, and John H. Seinfeld
Department of Chemical Engineering, California Institute of Technology, Pasadena, California, USA

Received 24 September 2004; revised 6 January 2005; accepted 26 January 2005; published 6 April 2005.

[1] Organic aerosols in general and secondary organic aerosol (SOA) in particular are known to contribute significantly to the atmospheric population of cloud condensation nuclei (CCN). However, current knowledge is limited with respect to the nature of this contribution. This study presents a series of experiments wherein the potential for biogenically derived SOA to act as CCN is explored. Five compounds were studied: four monoterpenes (α-pinene, β-pinene, limonene, and Δ^3-carene) and one terpenoid alcohol (terpinene-4-ol). In each case the aerosol formation was driven by the reaction of ozone with the biogenic precursor. The SOA produced in each experiment was allowed to age for several hours, during which CCN concentrations were periodically measured at four supersaturations: S = 0.27%, 0.32%, 0.54%, and 0.80%. The calculated relationships between particle dry diameter and critical supersaturation were found to fall in the range of previously reported data for single-component organic aerosols; of the systems studied, α-pinene SOA was the least CCN active, while limonene SOA exhibited the strongest CCN activity. Interestingly, the inferred critical supersaturation of the SOA products was considerably more sensitive to particle diameter than was found in previous studies. Furthermore, the relationships between particle size and critical supersaturation for the monoterpene SOA shifted considerably over the course of the experiments, with the aerosol becoming less hygroscopic over time. These results are consistent with the progressive oligomerization of the SOA.

Citation: VanReken, T. M., N. L. Ng, R. C. Flagan, and J. H. Seinfeld (2005), Cloud condensation nucleus activation properties of biogenic secondary organic aerosol, *J. Geophys. Res.*, *110*, D07206, doi:10.1029/2004JD005465.

1. Introduction

[2] Organic compounds are known to compose a significant fraction of the atmospheric aerosol population. Fine-particle organic mass fractions exceeding 80% have been observed in the Amazon Basin [e.g., *Roberts et al.*, 2002]; fractions greater than 50% were measured on both the eastern and western coasts of the United States [*Rivera-Carpio et al.*, 1996; *Novakov et al.*, 1997]. Organic compounds can significantly affect the hygroscopic properties of the aerosol [*Saxena et al.*, 1995] and have consistently been found in the population of cloud condensation nuclei (CCN) in the ambient atmosphere [e.g., *Novakov and Penner*, 1993; *Liu et al.*, 1996; *Rivera-Carpio et al.*, 1996; *Matsumoto et al.*, 1997; *Roberts et al.*, 2002]. However, the number of compounds and the complexity of the mixtures often found in an aerosol population have made it difficult to even identify a large fraction of the organic material present, much less predict how that material affects the activation properties of the particles.

0148-0227/05/2004JD005465

[3] In recent years, there have been numerous studies under controlled laboratory conditions exploring the potential for organic particles to act as CCN. Initial studies [*Cruz and Pandis*, 1997; *Corrigan and Novakov*, 1999; *Prenni et al.*, 2001; *Giebl et al.*, 2002] focused on single-component organic particles, primarily dicarboxylic acids. Results indicated that soluble organic acids generally act as predicted by Köhler theory as traditionally applied (that is, the activation properties can be predicted by assuming that the particle is fully dissociated throughout the activation process) but that the behavior of less soluble organic compounds (e.g., adipic acid and dioctylphthalate) was not adequately described by this approach. More recent studies have elaborated upon these results. *Cruz and Pandis* [1998] determined that organic coatings do not inhibit the activation of an inorganic core and that the ability of coated particles to act as CCN can be predicted by Köhler theory. *Raymond and Pandis* [2002] applied the results of *Shulman et al.* [1996] (who modified Köhler theory to include slightly soluble compounds) to observations of several additional organic compounds and noted that a compound's wettability as well as its solubility appear to affect its activation properties. *Kumar et al.* [2003] noted that as is

the case for some inorganic salts, the van't Hoff factor for organic compounds may vary as the droplet grows. Measurements by *Shantz et al.* [2003] demonstrated that in addition to modifying equilibrium behavior the presence of organic species can slow droplet growth. *Raymond and Pandis* [2003] examined a series of multicomponent organic particles, both internally mixed and coated particles, and found that activation behavior was again well predicted by the modified Köhler theory. Most recently, *Broekhuizen et al.* [2004] and *Bilde and Svenningsson* [2004] suggested that trace amounts of water or inorganic impurities would have sufficiently large effects on a particle's CCN activity to explain much of the variability in the earlier observations.

[4] While studying organic aerosols of known composition is the best way to resolve the outstanding issues when comparing observations with the theory of CCN activity, such simple compositions do not reflect the complexity of the organic component of the ambient aerosol population. It is possible to approach this complexity in a laboratory setting by studying the activation properties of secondary organic aerosol (SOA). SOA is formed when volatile organic compounds are oxidized to form less volatile products, which then condense into the aerosol phase. Many organic compounds found in the atmosphere, of both anthropogenic and biogenic origin, have been found to produce SOA [*Seinfeld and Pankow*, 2003].

[5] While the precursors that form SOA can be of either anthropogenic or biogenic origin, the latter are of more immediate interest with respect to the potential influence on the concentration of global cloud condensation nuclei. The atmospheric burden of biogenically derived SOA is less than that of sulfate aerosols [*Griffin et al.*, 1999], but SOA can be a primary source of fine aerosol mass (and hence CCN) in many remote locations, such as the Amazon Basin [*Roberts et al.*, 2002] and Scandinavian boreal forests [*Hämeri et al.*, 2001].

[6] To date, there have been few studies examining the hygroscopic properties of the SOA products of common biogenic precursors. *Virkkula et al.* [1999] used a tandem differential mobility analyzer to measure the hygroscopic growth factors of SOA produced from three biogenic monoterpenes: limonene, α-pinene, and β-pinene. They conducted experiments both with and without inorganic seed particles, and in each case the final calculated diameter growth factor was $\sim$1.1 at relative humidities of $\sim$85%; the measured values agreed with estimates that assumed that the water uptake of the organic and inorganic fractions was additive. *Cocker et al.* [2001a] and *Saathoff et al.* [2003] made similar measurements of the SOA products of α-pinene ozonolysis, with the same results. *Hegg et al.* [2001] presented very limited data for laboratory measurements of the CCN properties of SOA; their results indicate that the SOA products of cyclohexene oxidation are more prone to act as CCN than the products of α-pinene oxidation. As of the time of writing, additional studies of the SOA properties of CCN are at varying stages of completion.

[7] This paper presents the results of a series of laboratory experiments investigating the CCN activity of SOA produced by the ozonolysis of five common biogenic compounds: four monoterpenes (α-pinene, β-pinene, Δ^3-carene, and limonene) and one terpenoid alcohol (terpinene-4-ol). The chosen monoterpenes represent an estimated 85% of global monoterpene emissions, while the terpenoid alcohols make up $\sim$25% of the other biogenic compounds capable of forming SOA [*Griffin et al.*, 1999]. For each experiment, CCN concentrations are presented for at least three supersaturations; these data are compared to measured size distributions to derive the size–critical supersaturation relationship for SOA products of each biogenic compound. The derived relationships have unexpected characteristics, the possible causes of which are explored in some detail.

Table 1. Summary of Biogenic Ozonolysis Experiments

Date	Compound	Initial Hydrocarbon Concentration, ppb	Peak Particle Concentration, cm^{-3}
16 July	α-pinene	20	6150
25 July	limonene	5	3950
30 July	terpinene-4-ol	10	5730
9 August	β-pinene	10	2020
12 August	Δ^3-carene	10	5290

2. Experimental System

[8] The atmospheric reactions leading to SOA formation can be replicated under controlled conditions in the Caltech indoor facility, described in detail by *Cocker et al.* [2001b]. The facility comprises two 28-m^3 transparent, flexible, Teflon chambers. An extensive suite of gas phase and aerosol sampling instrumentation is connected to each chamber; of primary interest here are the CCN counter integrated into the facility for this study and the particle concentration and size distribution measurements.

[9] Prior to each of the experiments performed for this study the chamber was flushed with dry, particle-free, hydrocarbon-free air for several hours until the particle concentration in the chamber was sufficiently low (less than 20 cm^{-3}), and the concentrations of gas phase reactants (hydrocarbons, ozone, and NO_x) were below detection limits. Once the chamber was clean, the biogenic reactant was injected; the initial reactant concentration was chosen so that the number concentration of the SOA would be less than $\sim$6000 cm^{-3} (to minimize coincidence errors in the CCN counter). The initial reactant concentrations for each experiment can be found in Table 1. While these starting concentrations were chosen primarily to generate concentrations in the optimal range, they are also in the range of monoterpene concentrations observed in the southeastern United States during the Southern Oxidants Study [*Guenther et al.*, 1996].

[10] Approximately 1 hour was required for the hydrocarbon concentration to stabilize after the time of injection; the chamber was considered to be well mixed when the concentration was stable for several minutes. The aerosol instruments were started during this mixing period to allow sufficient warm-up time. Once the organic precursor had equilibrated, the reaction was initiated by injecting ozone in excess of the concentration required for complete reaction. Sufficient ozone was injected such that if no reaction were to occur, the ozone concentration would be approximately double that of the biogenic precursor (ozone concentrations of several parts per billion were typically observed when the experiments were terminated). Nucleation began a short time after ozone injection, but again, $\sim$1 hour elapsed before concentra-

Table 2. Summary of the Supersaturation Cycle for the Cloud Condensation Nucleus Counter

Step	ΔT,[a] K	S_{eff},[b] %	Duration, min:s	Stabilization Time, min:s	Measurement Time, min:s
1	0.2	0.27	40:00	25:00	15:00
2	0.4	0.32	26:40	10:00	16:40
3	2.0	0.54	26:40	10:00	16:40
4	5.0	0.80	25:00	10:00	15:00
Rewet	NA[c]	NA[c]	01:40	01:40	00:00

[a]Temperature gradient over the length of the column.
[b]Effective supersaturation of the cloud condensation nucleus counter, derived from an instrument calibration (Figure 1).
[c]NA, not applicable.

tions stabilized; observations during this period were not included in the analysis. After this equilibration period in each experiment the observed particle concentration reached a maximum and did not vary rapidly, indicating that the system was well mixed. Over the course of several hours the oxidation products continued to condense on the available particles, increasing the aerosol volume; eventually, the volume concentration also peaked and then began to decrease as particles were deposited on the chamber walls. Measurements of the gas phase concentrations and aerosol properties were made throughout this period from a point near the center of the bag; descriptions of the aerosol instrumentation used in this study follow in sections 2.1 and 2.2.

2.1. CCN Counter

[11] The CCN counter used in this work has been employed previously in various configurations during several field experiments [*Chuang et al.*, 2000; *VanReken et al.*, 2003; T. M. Sharon et al., Aerosol and cloud microphysical characteristics of rifts and gradients in maritime stratocumulus clouds, submitted to *Journal of the Atmospheric Sciences*, 2005]. The original instrument design and subsequent modifications are discussed in detail in the earlier work and are not repeated here. For this work the CCN counter has been upgraded to allow for completely autonomous operation over extended periods of time. The improvements to the growth chamber are essentially identical to those incorporated into the development of the three-column CCN instrument developed by T. Rissman et al. (manuscript in preparation, 2004) for airborne operation. As now configured, the CCN counter maintains a linear temperature at the wall of the growth column to impose a near-constant supersaturation along the centerline, a design first implemented successfully by *Roberts and Nenes* [2005]. To maintain the temperature profile, thermal masses controlled by pairs of thermoelectric coolers are located at the entrance and exit of the growth column, with an additional control point midway along the length of the column. To make the instrument more autonomous, software-controllable valves (Peter Paul solenoid control valves, models 52J8DGB-12VDC and 51J8XGB-12VDC) and temperature controllers (Wavelength Electronics model WTC3243) were incorporated into the instrument. During these experiments the instrument was operated at a total flow rate of 0.48 L min^{-1}, with a sheath-to-sample ratio of ~7:1; the sampling frequency was 0.5 Hz.

[12] The improved temperature control capability incorporated into the CCN counter allows for a new measurement strategy to be implemented. By periodically adjusting the imposed temperature gradient (ΔT) the instrument can be stepped through a series of gradually increasing supersaturations. While the temperatures at the control points stabilize fairly quickly (~20 s), empirical experience indicates that at least 10 min are required for the instrument to stabilize at a new supersaturation profile; the stabilization time depends on the magnitude of the temperature change. For this experiment the total cycle time was chosen to be 120 min; initially, the cycle was divided into four equal steps, but the results of the first experiment (α-pinene) indicated that this was insufficient stabilization time between the largest and smallest temperature gradients. For the remainder of the experiments the supersaturation cycle was modified to allow more sampling time at the smallest temperature gradient (Table 2).

[13] To determine the effective supersaturation (S_{eff}) of the CCN counter at each of the four selected temperature gradients, a series of instrument calibrations were performed. Particles of known composition were generated by atomizing an ammonium sulfate solution and passing the resulting particles through a diffusion dryer. A differential mobility analyzer was then used to select particles of a given size from the polydisperse distribution exiting the dryer; the result is a nearly monodisperse ammonium sulfate aerosol. These particles are sampled simultaneously by the CCN counter and by a condensation particle counter (CPC) (Thermo Systems Inc. (TSI) model 3010). By stepping through a series of median diameters and then measuring the ratio of particles measured by the CCN counter to those counted by the CPC (the ''activation ratio'') a response curve can be generated for the CCN counter at a given temperature gradient (Figure 1). The median diameters are converted to particle critical supersaturations using code developed by *Brechtel and Kreidenweis* [2000]. In two of the calibrations (for ΔT = 0.2 and 2.0 K), there was a small blockage in the entrance to the CCN counter's optical counter that removed a small fraction of the activated droplets prior to counting (less than 20%); to correct for this effect, the data in Figure 1 were normalized such that the largest activated fraction for each experiment is 1.0. It should be noted that the blockage was cleared after the calibration experiments and that the measured CCN concentration for large salt particles then agreed with the CPC; thereafter the droplet detector was cleaned prior to each experiment. On the basis of the calibration results the effective supersaturations for the four temperature gradients used in this study (ΔT = 0.2, 0.4, 2.0, and 5.0 K) are 0.27%, 0.32%, 0.54%, and 0.80%, respectively; in each case the

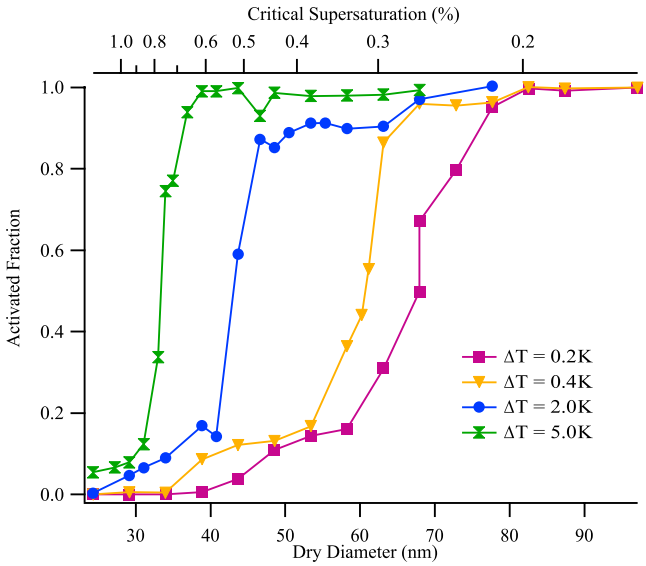

Figure 1. Cloud condensation nucleus (CCN) instrument calibrations at each of the four temperature gradients used in this study. Activated fractions are presented as a function of particle dry diameter and critical supersaturation. Data have been normalized as described in the text.

uncertainty in the effective supersaturation is estimated to be ~0.05%.

2.2. Particle Number and Aerosol Size Distribution

[14] In order to determine the relationship between particle size and critical supersaturation for the SOA studied here it is necessary to have detailed information about the aerosol size distribution in addition to the CCN data. Throughout these experiments, measurements of the aerosol size distribution were made using a scanning electrical mobility spectrometer (SEMS) (also known as a scanning mobility particle sizer), described by *Wang and Flagan* [1989]. *Cocker et al.* [2001b] described the operating conditions for the instrument used here; the size range for the instrument is approximately 15 nm < D_p < 775 nm, and size distributions were measured every 4 min. An additional measurement of the aerosol number concentration was made using a CPC (TSI model 3010).

[15] During the experiments the data revealed a systemic difference between the aerosol concentration measured by the CPC and the integrated size distribution from the SEMS, with the latter yielding a lower concentration (typically 12–16%). The difference persisted even when there were no particles at the low end of the size distribution, so it is unlikely that the discrepancy is due to particles below the detection limit for the SEMS. The CCN concentration also exceeded the total concentration from the SEMS in several of the experiments but never exceeded the particle concentration measured by the CPC by more than the measurement uncertainty. This strongly suggests that the SEMS measurement of particle concentration is in error; the SEMS data have therefore been corrected to be more consistent with the CPC data. The correction was calculated by finding the mean difference between the two instruments for each experiment after the peak number concentration had been reached; this scaling factor was then applied to each size bin of the SEMS data set at each time interval for that experiment. No extensive effort was made to determine the cause for the disagreement between the SEMS and the other aerosol instruments, but *Liu and Deschler* [2003] found that charge neutralizers like those used in the SEMS often fail to fully equilibrate the charge distribution of an aerosol population; this may explain the discrepancy.

[16] The relatively low particle concentrations produced in these experiments made another correction to the data from the SEMS necessary. In a scanning system, there is only a small effective measurement time at a given size; at low particle concentrations the concentration in each size bin is based on a small number of counted particles, which results in much greater statistical uncertainty. The result is noisy size spectra that complicate the comparison between the measurements of the SEMS and the CCN counter. To reduce the uncertainty associated with the limited counting

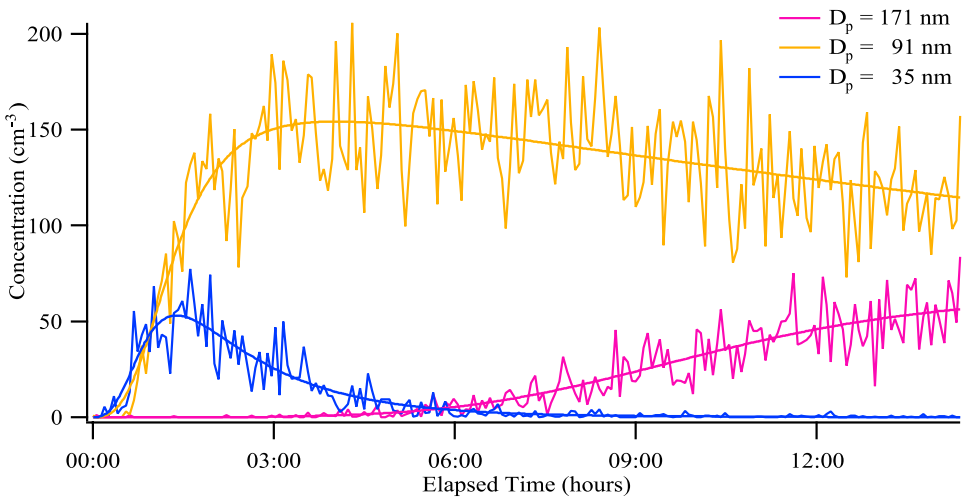

Figure 2. Examples of the curve fit used to smooth the scanning electrical mobility spectrometer (SEMS) data. Data are from the limonene experiment after the SEMS data were scaled to the condensation particle counter (CPC) data.

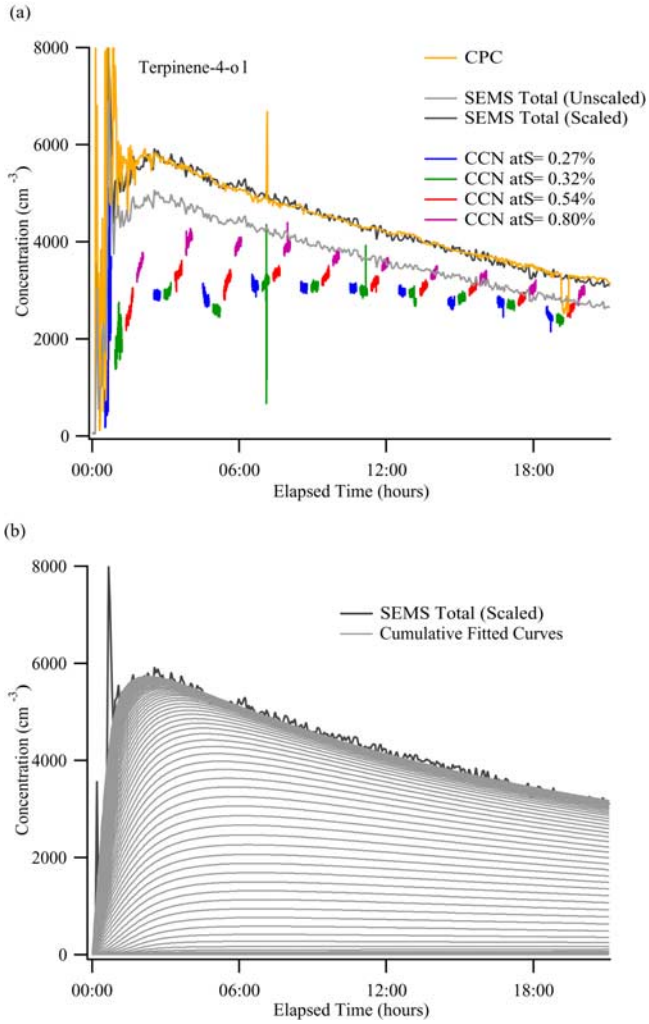

Figure 3. Time series data from the terpinene-4-ol experiment. (a) CCN data at each of the four supersaturations, total particles from the CPC, the unscaled total SEMS concentration, and the total SEMS concentration scaled to the CPC concentrations. (b) Cumulative size distribution time series, calculated from fitted curves as described in the text. The scaled total SEMS concentration is again included for comparison. By comparing the fitted cumulative size distributions to the measured CCN concentrations the relationship between particle size and critical supersaturation can be inferred.

statistics in the SEMS, the time series for each bin of the size distribution data has been replaced with a fitted curve that smoothly represents the time variation in the concentration within that size bin. The function used for the fit was chosen to generally represent the movement of particles into and out of a given size bin by combining the features of a sigmoidal change with an exponential decay. The function is

$$N(t) = \frac{N_\infty + Ae^{-Bt}}{1 + \left(\frac{t_0}{t}\right)^R}, \quad (1)$$

where $N(t)$ is the concentration of particles in a given size bin at time t. N_∞ is the concentration in the bin at large t, if there were no decay; A and B are the constants for the exponential decay. The transition that occurs as the concentration within the size bin first increases is expressed by the denominator of the fitting function; t_0 determines when the transition occurs, and R governs the rate of the transition.

[17] Equation (1) was used to fit the time series data from the SEMS across the range of particle diameters, even though the shape of these time series varies considerably across the range (Figure 2). The solution for the fit was obtained using the curve-fitting tool included in the Igor Pro data analysis software package (WaveMetrics, Inc.). The solution frequently did not converge neatly, so every fit was confirmed visually. After obtaining a good fit for each size bin the curves could be used to generate smooth size distributions, both differential and cumulative, for comparison with the CCN measurements.

3. Results and Discussion

[18] Each of the experiments was continued for at least 12 hours after the injection of ozone. The time series from the three instruments during the terpinene-4-ol experiment are presented in Figure 3a to demonstrate the relationship between the data sets. Early in the experiment, the rapid fluctuations in the observations are a result of incomplete mixing of the freshly nucleated particles in the chamber; as has been noted, the chamber is well mixed ~1 hour after the onset of nucleation. The peak in the CPC concentration occurs earlier than the peak SEMS concentration because the smallest particles had not yet grown into the SEMS size range. The offset between the particle concentration observed by the CPC and the (unscaled) total SEMS concentration is apparent and remains even after there are no longer any particles near the edges of the detection range for the SEMS. The scaled SEMS concentration matches closely with the CPC data for times after the SEMS has reached its peak concentration. Figure 3b shows the result of the curve-fitting procedure on the size distribution data. Each smooth curve is cumulative, representing the integrated size distribution from the top range down to the particle diameter represented by the curve. The lowest curve (nearest the x axis) is the fitted curve for the largest size bin in the SEMS data; the second curve is the sum of the largest two bins, the third curve is the sum of the largest three bins, and so on. The top curve, which is therefore the fitted curve for the fully integrated size distribution, closely follows the (scaled) total concentration measured by the SEMS, a good indication of the effectiveness of the curve-fitting process.

[19] Using the fitted size distributions (i.e., Figure 3b, smooth curves), it is possible to infer the relationship between particle size and critical supersaturation for the SOA at any time during the experiment. If the composition of the SOA is assumed to be constant over the breadth of the size distribution, then the particle diameter at which the integrated size distribution (from the top down) equals the measured CCN concentration has a critical supersaturation equal to the effective supersaturation of the CCN counter (hereinafter this diameter will be termed the "cut diameter"). Performing this calculation at each supersaturation during a 2-hour measurement cycle yields the

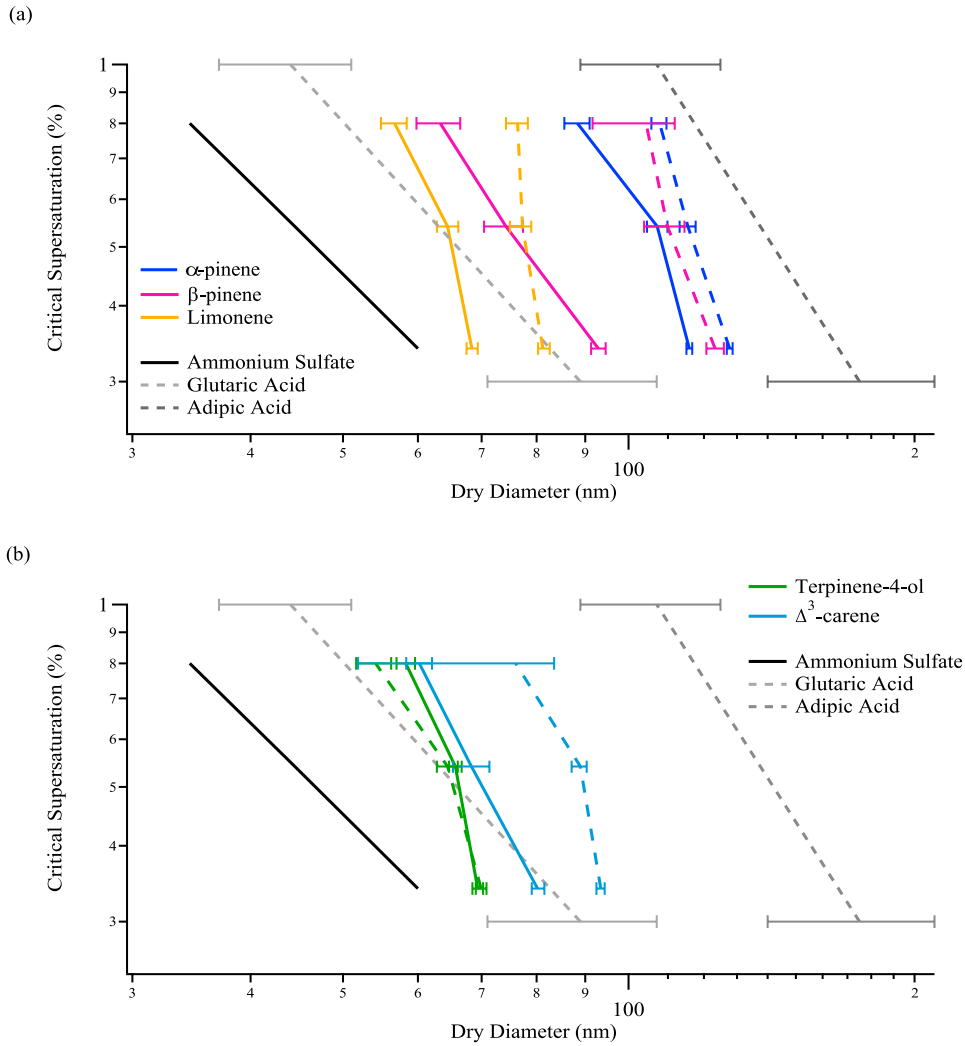

Figure 4. CCN response for secondary organic aerosol products of (a) α-pinene, β-pinene, and limonene and (b) Δ^3-carene and terpinene-4-ol. Compounds are coded by color. Solid lines are from the cycle immediately following the peak in the fitted SEMS concentration, and dashed lines are from the last cycle in each experiment. Error bars are as described in the text. Included for comparison are data for ammonium sulfate from the instrument calibration and measurements for glutaric and adipic acid from *Raymond and Pandis* [2002].

critical supersaturation as a function of particle diameter (Figure 4). The data in Figure 4 are for two cycles from each experiment: the first full cycle after the maximum in the integrated SEMS concentration and the last full cycle before the end of the experiment. For each point the CCN data were averaged over the length of a single measurement period (~15 min) (see Table 2); when the mean concentration fell between two bins of the size distribution, the diameter was calculated by linear interpolation. Error bars represent the change in diameter associated with a shift of one standard deviation in the CCN concentration; the uncertainty in the SEMS measurement is not considered. Also included in Figure 4 for comparison are the calculated relationship for ammonium sulfate used in the instrument calibration and measurements for adipic acid and glutaric acid from the study of *Raymond and Pandis* [2002]. Data recorded at S = 0.27% were very similar to the results at S = 0.34% and were therefore excluded from Figure 4 (it seems likely that even with the extended stabilization time the CCN counter did not always reach the intended setting of S = 0.27%).

[20] The curves for glutaric and adipic acid in Figure 4 are indicative of the range of CCN properties of low–molecular weight organic acids found in the atmosphere. The SOA products of the biogenic compounds studied here generally fall within this range. Considering for the moment only the data from early in each experiment, the products of the α-pinene oxidation are clearly the least likely to act as CCN (that is, they require the highest supersaturation for activation to occur); of the compounds studied, only α-pinene SOA exhibited behavior more like adipic acid than glutaric acid. The rest of the SOA products, in order of increasing CCN activity, are β-pinene, Δ^3-carene, terpinene-4-ol, and limonene.

[21] Somewhat surprisingly, the activation properties of the SOA generated in this study are extremely sensitive to

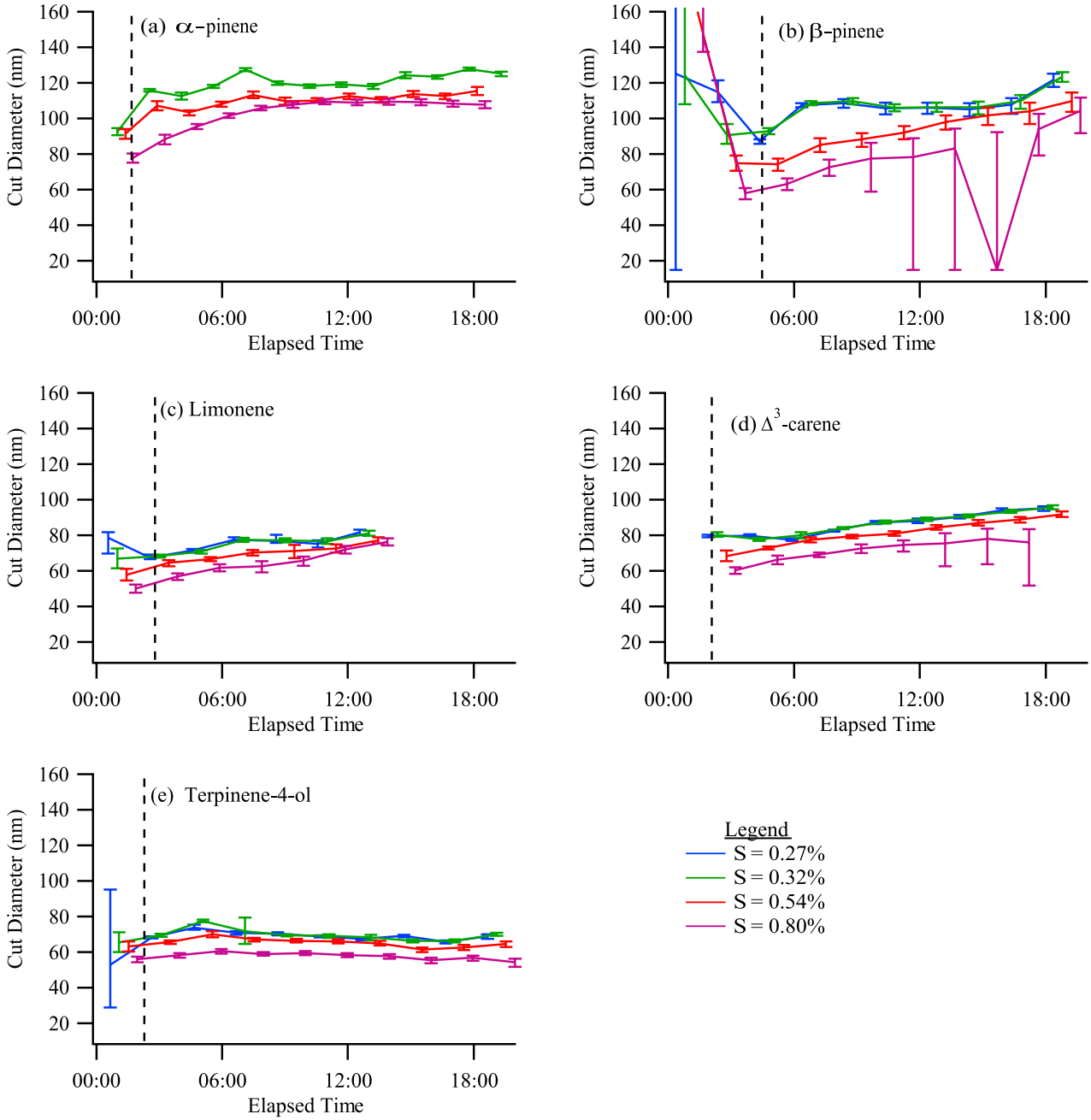

Figure 5. Time series for the calculated cutoff diameters at each of the four supersaturations for (a) α-pinene, (b) β-pinene, (c) limonene, (d) Δ^3-carene, and (e) terpinene-4-ol. In Figure 5b the measured CCN concentration at S = 0.80% is very close to the total SEMS concentration for three measurement periods; when the mean CCN concentration (or the mean plus the standard deviation) surpassed the SEMS total, the minimum diameter was used.

particle size; the same change in diameter produces a much greater change in critical supersaturation for the SOA than for the single-component aerosols. Classical Köhler theory predicts a slope similar to that observed for single-component aerosols by *Raymond and Pandis* [2002]; the ammonium sulfate line in Figure 4 is from theory and confirms the expected slope. Thus the cause of sensitivity observed in this study is not immediately clear. The presence of insoluble material in the SOA would shift the response curve toward larger particle sizes but would not be expected to significantly change the slope. Similarly, a decrease in surface tension of the growing droplets would shift the response curve toward smaller sizes but also would not change the slope. The presence of film-forming compounds [*Feingold and Chuang*, 2002] or slightly soluble compounds [*Shulman et al.*, 1996] could alter the slope of the size–critical supersaturation relationship, but the expected effect would be the opposite of that observed; the presence of such compounds impedes droplet growth, which may prevent CCN from

being properly counted. However, the effect would be greater at low supersaturations (where the driving force for growth is less) and would cause those data to be skewed toward larger diameters. Instead, the size–critical supersaturation relationship is skewed toward smaller diameters at low supersaturations. It is also possible that the steepness of the size–critical supersaturation relationship is an artifact resulting from a measurement bias, but there is no evidence that this was occurring.

[22] One characteristic that would at least partially explain the observed behavior is if the SOA becomes less hygroscopic as it ages. Indeed, there is substantial evidence that this is occurring; in each of the experiments save that of terpinolene-4-ol (the only nonmonoterpene studied) the CCN activity decreased significantly over the course of the experiment (Figure 4). The trend is consistent throughout the experiments, as can be seen in Figure 5, which displays the time series of the calculated cut diameters for each supersaturation of each experiment. The vertical dashed lines in Figure 5 denote the time that the integrated (fitted) size distribution reached its maximum value for the experiment; after that maximum is reached in each of the monoterpene experiments, there is a consistent trend over time toward reduced CCN activity. This trend, even with no knowledge of the cause, accounts for at least part of the steepness in the size–critical supersaturation relationships in Figure 4. Because the higher-supersaturation stages were at the end of each cycle, the values for the larger critical supersaturations in Figure 4 are skewed somewhat toward larger diameters than if all supersaturations had been measured simultaneously.

[23] These data strongly suggest that the composition of the monoterpene SOA is changing over the course of the experiments, with the SOA becoming less hygroscopic. It is known that SOA products can react further in the particle phase to form polymers [*Limbeck et al.*, 2003; *Kalberer et al.*, 2004; *Tolocka et al.*, 2004], and *Gao et al.* [2004] recently determined that oligomers with molecular weights greater than 200 are ubiquitous in SOA formed by α-pinene ozonolysis (oligomers are chains of two to four molecules and can be thought of as an intermediate step in the formation of a polymer). The temporal variations in the calculated cut diameters observed during these experiments are consistent with a progressive oligomerization of the SOA. Because of their high molecular weight and reduced polarity, oligomers are almost certainly less soluble than their precursors. Thus, as the aerosol ages, a larger particle would be required for the same soluble mass, which would result in a gradual increase in the cutoff diameter at a given supersaturation. This is the trend observed in Figure 5. Because of the timing of the measurement cycle (that is, in each cycle the higher supersaturation measurements followed those at lower supersaturations) a progressive oligomerization would also tend to increase the cutoff diameter for the higher supersaturations, skewing the slope of the data in Figure 4. Such reasoning does not fully explain the steepness observed in the aerosol size–critical supersaturation relationship, but in the presence of a potentially variable composition across the size spectrum it is not entirely surprising if the CCN concentration is relatively insensitive to supersaturation. In light of these results it may not be completely appropriate to describe the size–critical supersaturation relationship for SOA in terms of a single "cut diameter."

4. Conclusions

[24] The CCN activity of SOA produced from the ozonolysis of five common biogenic compounds was investigated. Measurements were made at several supersaturations ranging from $S = 0.27\%$ to $S = 0.80\%$. The SOA produced during the experiments exhibited CCN potential similar to previously examined single-component organic aerosols; of the compounds studied, SOA from limonene oxidation was the most CCN active, while α-pinene SOA was the least active. The observations were notable in that the critical supersaturation of SOA particles appeared to be much more strongly sensitive to particle diameter than is usual, and (with the exception of terpinene-4-ol SOA) the particles became significantly less active as CCN as they aged. These observations are consistent with gradual oligomerization occurring in the monoterpene SOA as it ages. These are among the first measurements of the CCN properties of laboratory-generated SOA; clearly, more study is required to fully understand the behavior presented here.

[25] **Acknowledgments.** This research was supported by the Office of Science (BER), U.S. Department of Energy, grant DE-FG02-01ER63099, and by U.S. Environmental Protection Agency grant RD-83107501-0. Although the research described in this article has been funded in part by the U.S. Environmental Protection Agency, it has not been subjected to the Agency's required peer and policy review and therefore does not necessarily reflect the view of the Agency, and no official endorsements should be inferred. The authors would like to thank R. Bahreini for assistance with the aerosol calibration system.

References

Bilde, M., and B. Svenningsson (2004), CCN activation of slightly soluble organics: The importance of small amounts of inorganic salt and particle phase, *Tellus, Ser. B*, *56*(2), 128–134.

Brechtel, F. J., and S. M. Kreidenweis (2000), Predicting particle critical supersaturation from hygroscopic growth measurements in the humidified TDMA. Part I: Theory and sensitivity studies, *J. Atmos. Sci.*, *57*(12), 1854–1871.

Broekhuizen, K., P. P. Kumar, and J. P. D. Abbatt (2004), Partially soluble organics as cloud condensation nuclei: Role of trace soluble and surface active species, *Geophys. Res. Lett.*, *31*, L01107, doi:10.1029/2003GL018203.

Chuang, P. Y., D. R. Collins, H. Pawlowska, J. R. Snider, H. H. Jonsson, J.-L. Brenguier, R. C. Flagan, and J. H. Seinfeld (2000), CCN measurements during ACE-2 and their relationship to cloud microphysical properties, *Tellus, Ser. B*, *52*(2), 843–867.

Cocker, D. R., S. L. Clegg, R. C. Flagan, and J. H. Seinfeld (2001a), The effect of water on gas-particle partitioning of secondary organic aerosol. Part I: Alpha-pinene/ozone system, *Atmos. Environ.*, *35*(35), 6049–6072.

Cocker, D. R., R. C. Flagan, and J. H. Seinfeld (2001b), State-of-the-art chamber facility for studying atmospheric aerosol chemistry, *Environ. Sci. Technol.*, *35*(12), 2594–2601.

Corrigan, C. E., and T. Novakov (1999), Cloud condensation nucleus activity of organic compounds: A laboratory study, *Atmos. Environ.*, *33*(17), 2661–2668.

Cruz, C. N., and S. N. Pandis (1997), A study of the ability of pure secondary organic aerosol to act as cloud condensation nuclei, *Atmos. Environ.*, *31*(15), 2205–2214.

Cruz, C. N., and S. N. Pandis (1998), The effect of organic coatings on the cloud condensation nuclei activation of inorganic atmospheric aerosol, *J. Geophys. Res.*, *103*(D11), 13,111–13,123.

Feingold, G., and P. Y. Chuang (2002), Analysis of the influence of film-forming compounds on droplet growth: Implications for cloud microphysical processes and climate, *J. Atmos. Sci.*, *59*(12), 2006–2018.

Gao, S., M. Keywood, N. L. Ng, J. Surratt, V. Varutbangkul, R. Bahreini, R. C. Flagan, and J. H. Seinfeld (2004), Low-molecular-weight and oligomeric components in secondary organic aerosol from the ozonolysis of cycloalkenes and α-pinene, *J. Phys. Chem. A*, *108*(46), 10,147–10,164.

Giebl, H., A. Berner, G. Rieschl, H. Puxbaum, A. Kasper-Giebl, and R. Hitzenberger (2002), CCN activation of oxalic and malonic acid test aerosols with the University of Vienna cloud condensation nuclei counter, *J. Aerosol Sci.*, *33*(12), 1623–1634.

Griffin, R. J., D. R. Cocker, and J. H. Seinfeld (1999), Estimate of global atmospheric organic aerosol from oxidation of biogenic hydrocarbons, *Geophys. Res. Lett.*, *26*(17), 2721–2724.

Guenther, A., P. Zimmerman, L. Klinger, J. Greenberg, C. Ennis, K. Davis, and W. Pollock (1996), Estimates of regional natural volatile organic compound fluxes from enclosure and ambient measurements, *J. Geophys. Res.*, *101*(D1), 1345–1359.

Hämeri, K., M. Väkevä, P. P. Aalto, M. Kulmala, E. Swietlicki, J. Zhou, W. Seidl, E. Becker, and C. D. O'Dowd (2001), Hygroscopic and CCN properties of aerosol particles in boreal forests, *Tellus, Ser. B*, *53*(4), 359–379.

Hegg, D. A., S. Gao, W. Hoppel, G. Frick, P. Caffrey, W. R. Leaitch, N. Shantz, J. Ambrusko, and T. Albrechcinski (2001), Laboratory studies of the efficiency of selected organic aerosols as CCN, *Atmos. Res.*, *58*(3), 155–166.

Kalberer, M., et al. (2004), Identification of polymers as major components of atmospheric organic aerosols, *Science*, *303*(5664), 1659–1662.

Kumar, P. P., K. Broekhuizen, and J. P. D. Abbatt (2003), Organic acids as cloud condensation nuclei: Laboratory studies of highly soluble and insoluble species, *Atmos. Chem. Phys.*, *3*, 509–520.

Limbeck, A., M. Kulmala, and H. Puxbaum (2003), Secondary organic aerosol formation in the atmosphere via heterogeneous reaction of gaseous isoprene on acidic particles, *Geophys. Res. Lett.*, *30*(19), 1996, doi:10.1029/2003GL017738.

Liu, P. S. K., and T. Deschler (2003), Causes of concentration differences between a scanning mobility particle sizer and a condensation particle counter, *Aerosol Sci. Technol.*, *37*(11), 916–923.

Liu, P. S. K., W. R. Leaitch, C. M. Banic, S.-M. Li, D. Ngo, and W. J. Megaw (1996), Aerosol observation at Chebogue Point during the 1993 North Atlantic Regional Experiment: Relationships among cloud condensation nuclei, size distribution, and chemistry, *J. Geophys. Res.*, *101*(D22), 28,971–28,990.

Matsumoto, K., H. Tanaka, I. Nagao, and Y. Ishizaka (1997), Contribution of particulate sulfate and organic carbon to cloud condensation nuclei in the marine atmosphere, *Geophys. Res. Lett.*, *24*(6), 655–658.

Novakov, T., and J. E. Penner (1993), Large contribution of organic aerosols to cloud-condensation-nuclei concentrations, *Nature*, *365*(6449), 823–826.

Novakov, T., D. A. Hegg, and P. V. Hobbs (1997), Airborne measurements of carbonaceous aerosol on the East Coast of the United States, *J. Geophys. Res.*, *102*(D25), 30,023–30,030.

Prenni, A. J., P. J. DeMott, S. M. Kreidenweis, D. E. Sherman, L. M. Russell, and Y. Ming (2001), The effects of low molecular weight dicarboxylic acids on cloud formation, *J. Phys. Chem. A*, *105*(50), 11,240–11,248.

Raymond, T. M., and S. N. Pandis (2002), Cloud activation of single-component organic aerosol particles, *J. Geophys. Res.*, *107*(D24), 4787, doi:10.1029/2002JD002159.

Raymond, T. M., and S. N. Pandis (2003), Formation of cloud droplets by multicomponent organic particles, *J. Geophys. Res.*, *108*(D15), 4469, doi:10.1029/2003JD003503.

Rivera-Carpio, C. A., C. E. Corrigan, T. Novakov, J. E. Penner, C. F. Rogers, and J. C. Chow (1996), Derivation of contributions of sulfate and carbonaceous aerosols to cloud condensation nuclei from mass size distributions, *J. Geophys. Res.*, *101*(D14), 19,483–19,493.

Roberts, G. C., and A. Nenes (2005), A continuous-flow longitudinal thermal-gradient CCN chamber for airborne measurements, *Aerosol Sci. Technol.*, in press.

Roberts, G. C., P. Artaxo, J. Zhou, E. Swietlicki, and M. O. Andreae (2002), Sensitivity of CCN spectra on chemical and physical properties of aerosol: A case study from the Amazon Basin, *J. Geophys. Res.*, *107*(D20), 8070, doi:10.1029/2001JD000583.

Saathoff, H., K. H. Naumann, M. Schnaiter, W. Schock, O. Mohler, U. Schurath, E. Weingartner, M. Gysel, and U. Baltensparger (2003), Coating of soot and $(NH_4)_2SO_4$ particles by ozonolysis products of alpha-pinene, *J. Aerosol Sci.*, *34*(10), 1297–1321.

Saxena, P., L. M. Hildemann, P. H. McMurray, and J. H. Seinfeld (1995), Organics alter hygroscopic behavior of atmospheric particles, *J. Geophys. Res.*, *100*(D9), 18,755–18,770.

Seinfeld, J. H., and J. F. Pankow (2003), Organic atmospheric particulate material, *Annu. Rev. Phys. Chem.*, *54*, 121–140.

Shantz, N. C., W. R. Leaitch, and P. F. Caffrey (2003), Effect of organics of low solubility on the growth rate of small droplets, *J. Geophys. Res.*, *108*(D5), 4168, doi:10.1029/2002JD002540.

Shulman, M. L., M. C. Jacobson, R. J. Charlson, R. E. Synovec, and T. E. Young (1996), Dissolution behavior and surface tension effects of organic compounds in nucleating cloud droplets, *Geophys. Res. Lett.*, *23*(3), 277–280.

Tolocka, M. P., M. Jang, J. M. Ginter, F. J. Cox, R. M. Kamens, and M. V. Johnston (2004), Formation of oligomers in secondary organic aerosol, *Environ. Sci. Technol.*, *38*(5), 1428–1434.

VanReken, T. M., T. A. Rissman, G. C. Roberts, V. Varutbangkul, H. H. Jonsson, R. C. Flagan, and J. H. Seinfeld (2003), Toward aerosol/cloud condensation nucleus (CCN) closure during CRYSTAL-FACE, *J. Geophys. Res.*, *108*(D20), 4633, doi:10.1029/2003JD003582.

Virkkula, A., R. Van Dingenen, F. Raes, and J. Hjorth (1999), Hygroscopic properties of aerosol formed by oxidation of limonene, α-pinene, and β-pinene, *J. Geophys. Res.*, *104*(D3), 3569–3579.

Wang, S. C., and R. C. Flagan (1989), Scanning electrical mobility spectrometer, *J. Aerosol Sci.*, *20*(8), 1485–1488.

R. C. Flagan, N. L. Ng, and J. H. Seinfeld, Department of Chemical Engineering, California Institute of Technology, Pasadena, CA 91125, USA. (seinfeld@caltech.edu)

T. M. VanReken, National Center for Atmospheric Research, Boulder, CO 80307, USA.